Spin-dependent recombination and hyperfine interaction at deep defects

E. L. Ivchenko, L. A. Bakaleinikov, and V. K. Kalevich
Ioffe Physical-Technical Institute, 194021 St. Petersburg, Russia
(Received 14 December 2014; revised manuscript received 3 April 2015; published 11 May 2015)

We present a theoretical study of optical electron-spin orientation and spin-dependent Shockley-Read-Hall recombination in the longitudinal magnetic field, taking into account the hyperfine coupling between the bound-electron spin and the nuclear spin of a deep paramagnetic center. The master rate equations for the coupled system are extended to describe the nuclear spin relaxation by using two distinct relaxation times, τ_{n1} and τ_{n2}, respectively, for defect states with one and two (singlet) bound electrons. The general theory is developed for an arbitrary value of the nuclear spin I. The magnetic-field and excitation-power dependencies of the electron and nuclear spin polarizations are calculated for the value of $I = 1/2$. In this particular case the nuclear effects can be taken into account by a simple replacement of the bound-electron spin relaxation time by an effective time dependent on free-electron and hole densities and free-electron spin polarization. The role of nuclear spin relaxation is visualized by isolines of the electron spin polarization on a two-dimensional graph with the axes $\log_2(\tau_{n1})$ and $\log_2(\tau_{n2})$.

DOI: 10.1103/PhysRevB.91.205202 PACS number(s): 71.70.Jp, 72.20.Jv, 72.25.Fe, 78.20.Bh

I. INTRODUCTION

Spin-dependent recombination (SDR) via deep paramagnetic centers has recently attracted great interest and been proven to be an effective tool for obtaining an abnormally high spin polarization of free and bound electrons in nonmagnetic semiconductor alloys $GaAs_{1-x}N_x$ and $Ga_{1-y}In_yAs_{1-x}N_x$ and quantum wells Ga(In)AsN/GaAs at room temperature [1–6] (see also Ref. [7] and references therein). The centers occupied by single spin-polarized electrons act as a spin filter [7–9] and block the free electrons of the same spin polarization escaping from the conduction band. As a result, the spin polarization of free photoelectrons generated by circularly polarized optical excitation (as well as that of bound electrons) can be enhanced up to $\sim 100\%$. The amplification of spin polarization is accompanied by an increase in the concentration of photoelectrons, the intensity of band-to-band photoluminescence (PL), and the photoconductivity, as compared to the linearly polarized photoexcitation [1,3,4,10].

The hyperfine interaction between the localized electron and the nucleus of the deep center mixes their spin states resulting in (i) a reduction of the initial electron spin polarization and (ii) dynamic nuclear polarization of the defect atoms [11]. In the absence of an external magnetic field, the localized-electron spin polarization can be reduced down to $1/2$ and $3/8$ for the nuclear spins $I = 1/2$ and $3/2$, respectively. The longitudinal magnetic field suppresses the hyperfine coupling and restores the electronic polarization as soon as the electron Zeeman energy exceeds the hyperfine interaction: the expected increase in the intensity and the circular polarization of the edge PL in the longitudinal magnetic field has been confirmed experimentally. In addition, strong nuclear polarization effects, due to a combination of the spin-dependent recombination and hyperfine coupling, have been reported and discussed in Refs. [12–19]. Particularly, the dynamically polarized nuclei create an effective magnetic field (the Overhauser field) acting on the spins of localized electrons; this field is added to the external magnetic field and shifts the "electron polarization vs field" curve, with the shift changing the sign under reversal of the circular polarization of the exciting light [13,14,17].

The theory of spin-dependent Shockley-Read-Hall recombination derived in Ref. [2] (for more details, see Ref. [7]) ignores the nuclear effects. It has been successfully applied to describe the main features of optical spin orientation of conduction-band and deep-level electrons in GaAsN at zero and transverse magnetic field $\boldsymbol{B} \perp z$, where the axis z is parallel to the exciting light beam and coincides with the normal to the sample surface. The model of Ref. [2] is unable to interpret the experimental data obtained in the longitudinal magnetic field $\boldsymbol{B} \parallel z$. The initial way out [13] was to assume the spin-relaxation time τ_{sc} of bound electrons to depend on the magnetic field B_z. This assumption could explain the polarization recovery with increasing the field. However, the modified model was not supported by a clear interpretation of the field dependence of τ_{sc}. Moreover, the modified model could not provide a reasonable interpretation of the observed shift of the polarization-field curve changing the sign under the reversal of circular polarization of the incident light.

The first attempt to give a theoretical description of the studied nuclear polarization processes was performed by Puttisong *et al.* [17] (see Supplementary Methods for Ref. [17]). In that work, the hyperfine interaction is taken into account approximately by introducing magnetic-field-independent flip-flop processes in the electron-nuclear system and including an additional phenomenological parameter, the flip-flop spin relaxation time. This approximation obviously provides physical insight into the role of the nuclei but its validity for a quantitative description is not obvious. A kinetic theory of the spin-dependent recombination incorporating the hyperfine interaction of electronic and nuclear spins has been proposed recently by Sandoval-Santana *et al.* [19]. The master equation approach for the spin-density matrix of the electron-nuclear system includes 144 equations which are solved numerically. The numerical calculation reproduces the main experimental findings of Ref. [14]. Nevertheless, the role of spin relaxation of nuclei in the system under consideration still remains open. In Ref. [19] the nuclear spins are polarized only in the deep-center states with single bound electrons. The defects with two bound electrons are characterized just by their

steady-state average concentration N_2. This means nothing more than that the formulation of Ref. [19] is based on the assumption of very fast nuclear spin relaxation in the defect state with a pair of electrons. As far as we know, at present there are no grounds to take this assumption for granted. In general the nuclear spin relaxation times τ_{n1} and τ_{n2} for defect states with one and two bound electrons can be of the same order and even longer than the lifetimes of these states.

In this work we develop a theory of the spin-dependent recombination and hyperfine coupling for the arbitrary values of τ_{n1} and τ_{n2} and analyze the role of each of them. The paper is organized as follows. In Sec. II we introduce the electron-nuclear spin-density matrix of the defect state with a single bound electron and the spin-density matrix of the defect with two bound electrons (in the singlet state) and discuss the restrictions imposed on the nonzero components of these matrices by the axial symmetry of the system in the longitudinal magnetic field. In Sec. III, we derive the rate equations for the spin density matrices taking into account both the hyperfine coupling for a nucleus with the angular momentum I and the electron and nuclear spin relaxation. The particular limiting cases are analyzed in Secs. III A and III B. The simplifications in the case of a nucleus with $I = 1/2$ are considered in Sec. IV. The results and discussion of the numerical calculations are presented in Sec. V. Section VI contains the concluding remarks.

II. ELECTRON-NUCLEAR SPIN-DENSITY MATRIX

We use the basic states $|s,m\rangle$ of the electron-nuclear system, where $s = \pm 1/2$ and m ($-I \leqslant m \leqslant I$) are the bound-electron and nuclear spin projections upon the fixed axis z, hereafter the normal to the sample surface, and I is the angular momentum of a nucleus. In the first, general part of the paper we take I to be arbitrary and then shift to the particular case of $I = 1/2$, which allows simplification of the kinetic equations for the densities and spin polarizations of the free and bound electrons. For the deep Ga_i^{2+}-interstitial defect responsible for the spin-dependent recombination in $GaAs_{1-x}N_x$ [12], the momentum I is 3/2. A detailed analysis for this value of I will be performed elsewhere.

In addition to $|s,m\rangle$, we also use the notation $|s,M-s\rangle$ for the state with the electron spin s and the total component of the angular momentum $M = s + m$. In the following we take into account the hyperfine interaction of the electron and nuclear spins given by the Fermi contact Hamiltonian

$$\mathcal{H}_{\rm hf} = A\boldsymbol{s}\cdot\boldsymbol{I},$$

where s_α and I_α ($\alpha = x,y,z$) are the electron and nuclear spin operators. Moreover, we consider the normal incidence of the polarized exciting light in the external magnetic field $\boldsymbol{B} \parallel z$ (Faraday geometry), take into account the Zeeman Hamiltonian $\mathcal{H}_{\boldsymbol{B}} = g\mu_B B_z s_z$ for the bound electrons, and neglect the interaction between the magnetic field and the magnetic moments of the nuclei and conduction-band electrons. Here the bound-electron Landé factor $g \approx 2$ and μ_B is the Bohr magneton.

The occupation of the defect with one bound electron is described by a $2(2I+1)\times 2(2I+1)$ spin-density matrix $\rho_{sm,s'm'}$. In the Faraday geometry, the components with unequal total angular-momentum components $M = s + m$ and $M' = s' + m'$ vanish. Therefore, it is enough to consider the components

$$\rho_{s,M-s;s',M-s'} \equiv \rho_{ss'}^{(M)}, \tag{1}$$

which are normalized on the density of single-electron defects

$$\sum_{s,m}\rho_{sm,sm} = \sum_{sM}\rho_{ss}^{(M)} = N_1\,.$$

The matrix $\rho_{ss'}^{(M)}$ with $M = I + 1/2$ or $M = -(I+1/2)$ contains only one nonzero component and can be presented as

$$\rho_{ss'}^{(I+\frac{1}{2})} = \delta_{ss'}\delta_{s,\frac{1}{2}}\rho_{\frac{1}{2},I;\frac{1}{2},I} \quad \text{and}$$
$$\rho_{ss'}^{(-I-\frac{1}{2})} = \delta_{ss'}\delta_{s,-\frac{1}{2}}\rho_{-\frac{1}{2},-I;-\frac{1}{2},-I}.$$

It is worth noting that the electron spin-density matrix (2×2 matrix)

$$\rho_{ss'}^{e} = \sum_{M}\rho_{ss'}^{(M)} \tag{2}$$

is diagonal, whereas the matrices $\rho_{ss'}^{(M)}$ with $|M| < I + 1/2$ contain off-diagonal components. In the geometry under consideration, the spin-density matrix of the defect singlet with two bound electrons is diagonal; its $2I+1$ diagonal components $N_{2,m}$ are normalized on the density of double-electron defects, N_2. The sum of N_1 and N_2 gives the density of deep defects, N_c.

Thus, for a nucleus with $I = 3/2$, instead of the 144 equations declared in Ref. [19], there are only 21 nonzero quantities to be found: 2 components $\rho_{1/2,1/2}^{(2)}$ and $\rho_{-1/2,-1/2}^{(-2)}$, 12 components $\rho_{ss'}^{(M)}$ with $M = 0, \pm 1$ and $s,s' = \pm 1/2$, four components $N_{2,m}$ with $m = \pm 3/2, \pm 1/2$, the densities of electrons $n_{\pm 1/2} \equiv n_\pm$ in the conduction band with the spin $\pm 1/2$, and the unpolarized free-hole density p.

III. KINETIC EQUATIONS FOR THE SPIN-DENSITY MATRIX

The following two kinetic equations,

$$2c_n N_- n_+ + \frac{n_+ - n_-}{2\tau_s} = G_+, \tag{3}$$

$$2c_n N_+ n_- + \frac{n_- - n_+}{2\tau_s} = G_-, \tag{4}$$

have the same form as those in the model of Ref. [7] where the hyperfine coupling was ignored. Here $N_+ = \rho_{1/2,1/2}^{e}$ and $N_- = \rho_{-1/2,-1/2}^{e}$ are the densities of single-electron defects with the electron spin $\pm 1/2$, their sum $N_+ + N_-$ being N_1; G_+ and G_- are the generation rates of the spin-up and spin-down photoelectrons; and c_n is the proportionality constant in the electron trapping rate by deep centers. We remind the reader that, due to the relations

$$N_+ + N_- + N_2 \equiv N_1 + N_2 = N_c\,, \tag{5}$$

$$p = n + N_2, \quad n = n_+ + n_-\,, \tag{6}$$

among the four densities n, N_1, N_2, and p, only two are linearly independent.

The steady-state kinetics of defects with two paired electrons is described by the $2I+1$ equations

$$(\dot{N}_{2,m})_{\rm cb} + (\dot{N}_{2,m})_{\rm vb} + (\dot{N}_{2,m})_{\rm sr} = 0\,. \tag{7}$$

The first term

$$(\dot{N}_{2,m})_{\rm cb} = 2c_n\left(n_-\rho^{(m+\frac{1}{2})}_{\frac{1}{2},\frac{1}{2}} + n_+\rho^{(m-\frac{1}{2})}_{-\frac{1}{2},-\frac{1}{2}}\right)$$

describes the generation of the defect states with two electrons due to the capture of a conduction-band electron on a single-electron defect. The second term

$$(\dot{N}_{2,m})_{\rm vb} = -c_p\,p N_{2,m}$$

describes the recombination of a free unpolarized photohole with one of the singlet-state electrons; c_p is the proportionality constant. The final term describes the nuclear spin relaxation. For the nuclei with $I = 1/2$ it has a simple unambiguous form:

$$(\dot{N}_{2,m})_{\rm sr} = -\frac{N_{2,m} - N_{2,-m}}{2\tau_{n2}} = -\frac{1}{\tau_{n2}}\left(N_{2,m} - \frac{N_2}{2}\right). \tag{8}$$

In the case of $I = 3/2$, the spin-relaxation term is ambiguous. However, if the perturbation leading to the inter-sublevel mixing is nonselective then, similarly to Eq. (8), the relaxation for $I = 3/2$ is characterized by one time parameter as follows [11]:

$$\begin{aligned}(\dot{N}_{2,m})_{\rm sr} &= -\frac{1}{\tau_{n2}}\left(N_{2,m} - \frac{1}{2I+1}\sum_{m'} N_{2,m'}\right)\\ &= -\frac{1}{\tau_{n2}}\left(N_{2,m} - \frac{N_2}{2I+1}\right).\end{aligned} \tag{9}$$

The kinetic equations for the spin-density matrices $\rho^{(M)}_{ss'} = \rho_{sm,s'm'}$ $(s+m = s'+m' = M)$ can be written in a compact form as

$$\dot{\hat{\rho}}^{(M)}_{\rm cb} + \dot{\hat{\rho}}^{(M)}_{\rm vb} + \dot{\hat{\rho}}^{(M)}_{\rm esr} + \dot{\hat{\rho}}^{(M)}_{\rm nsr} = \frac{\rm i}{\hbar}[\mathcal{H}^{(M)}\hat{\rho}^{(M)}]. \tag{10}$$

In Eq. (10) the first and second terms

$$\begin{aligned}\left(\dot{\rho}^{(M)}_{ss'}\right)_{\rm cb} &= -c_n(n_{-s} + n_{-s'})\rho^{(M)}_{ss'} \text{ and}\\ \left(\dot{\rho}^{(M)}_{ss'}\right)_{\rm vb} &= \frac{c_p}{2}N_{2,M-s}\,p\,\delta_{ss'}\end{aligned} \tag{11}$$

describe the capture and loss of the second electron by a defect. The term on the right-hand side represents the hyperfine and Zeeman interactions with a 2×2 M-dependent spin Hamiltonian:

$$\begin{aligned}\mathcal{H}^{(M)} &= \hbar(u_M s_z + v_M s_x)\,, \quad u_M = \beta + M\Omega\,,\\ v_M &= \Omega\sqrt{\left(I+\frac{1}{2}\right)^2 - M^2}\,,\end{aligned} \tag{12}$$

where $\Omega = A/\hbar$, $\beta = g\mu_B B_z/\hbar$, $s_\alpha = \sigma_\alpha/2$, and σ_α are the spin Pauli matrices. The bound-electron spin relaxation is phenomenologically described by the standard term

$$(\dot{\rho}_{sm,s'm'})_{\rm esr} = -\frac{1}{\tau_{sc}}\left(\rho_{sm,s'm'} - \frac{\delta_{ss'}}{2}\sum_{s''}\rho_{s''m,s''m}\right),$$

which is equivalent to

$$\left(\dot{\rho}^{(M)}_{ss'}\right)_{\rm esr} = -\frac{1}{\tau_{sc}}\left[\rho^{(M)}_{ss'} - \frac{\delta_{ss'}}{2}\left(\rho^{(M)}_{ss} + \rho^{(M-2s)}_{-s,-s}\right)\right]. \tag{13}$$

Similarly to Eqs. (8) and (9), the nuclear spin relaxation can simply be described by

$$(\dot{\rho}_{sm,s'm'})_{\rm nsr} = -\frac{1}{\tau_{n1}}\left(\rho_{sm,s'm'} - \frac{\delta_{mm'}}{2I+1}\sum_{m''}\rho_{sm'',sm''}\right), \tag{14}$$

or [see Eq. (2)]

$$\left(\dot{\rho}^{(M)}_{ss'}\right)_{\rm nsr} = -\frac{1}{\tau_{n1}}\left(\rho^{(M)}_{ss'} - \delta_{ss'}\frac{\rho^e_{ss}}{2I+1}\right). \tag{15}$$

We remind the reader that, for nonzero density-matrix components, the sum $s+m$ coincides with $s'+m'$, which means that $s = s'$ if $m = m'$. The set of matrix equations (10) represents $8I+2$ scalar equations, particularly, 6 equations for $I = 1/2$ and 14 equations for $I = 3/2$.

The summation of the terms in Eq. (10) over M yields the equations for the densities $N_\pm$ of single-electron defects [see Eqs. (3) and (4)]:

$$\begin{aligned}2c_n N_+ n_- + \frac{N_+ - N_-}{2\tau_{sc}} + \frac{\rm i}{\hbar}\sum_M[\mathcal{H}^{(M)}\hat{\rho}^{(M)}]_{\frac{1}{2},\frac{1}{2}} &= \frac{c_p}{2}N_2 p,\\ 2c_n N_- n_+ + \frac{N_- - N_+}{2\tau_{sc}} + \frac{\rm i}{\hbar}\sum_M[\mathcal{H}^{(M)}\hat{\rho}^{(M)}]_{-\frac{1}{2},-\frac{1}{2}} &= \frac{c_p}{2}N_2 p.\end{aligned} \tag{16}$$

The off-diagonal components of the spin-density matrix $\hat{\rho}^{(M)}$ can be expressed via the diagonal components:

$$\rho^{(M)}_{\frac{1}{2},-\frac{1}{2}} = \frac{\rm i}{\hbar}\frac{\mathcal{H}^{(M)}_{\frac{1}{2},-\frac{1}{2}}\left(\rho^{(M)}_{\frac{1}{2},\frac{1}{2}} - \rho^{(M)}_{-\frac{1}{2},-\frac{1}{2}}\right)}{c_n n + \frac{1}{\tau_{sc}} + \frac{1}{\tau_{n1}} + \frac{\rm i}{\hbar}\left(\mathcal{H}^{(M)}_{\frac{1}{2},\frac{1}{2}} - \mathcal{H}^{(M)}_{-\frac{1}{2},-\frac{1}{2}}\right)}. \tag{17}$$

Excluding the off-diagonal components we obtain for the diagonal components of the commutator in Eq. (10)

$$\begin{aligned}\frac{\rm i}{\hbar}[\mathcal{H}^{(M)}\hat{\rho}^{(M)}]_{\frac{1}{2},\frac{1}{2}} &= \frac{\rm i}{\hbar}\left(\mathcal{H}^{(M)}_{\frac{1}{2},-\frac{1}{2}}\rho^{(M)}_{-\frac{1}{2},\frac{1}{2}} - \rho^{(M)}_{\frac{1}{2},-\frac{1}{2}}\mathcal{H}^{(M)}_{-\frac{1}{2},\frac{1}{2}}\right)\\ &= U_M\left(\rho^{(M)}_{\frac{1}{2},\frac{1}{2}} - \rho^{(M)}_{-\frac{1}{2},-\frac{1}{2}}\right),\end{aligned} \tag{18}$$

where

$$U_M = \frac{1}{2}\frac{v_M^2 T_{cn}}{1 + u_M^2 T_{cn}^2} \tag{19}$$

and

$$\frac{1}{T_{cn}} = c_n n + \frac{1}{\tau_{sc}} + \frac{1}{\tau_{n1}}. \tag{20}$$

The factor U_0 is an even function of the longitudinal magnetic field, whereas the factors U_M with $M \neq 0$ are asymmetric functions of B_z because

$$u_M^2 = (\beta + M\Omega)^2 = (g\mu_B B_z + MA)^2/\hbar^2. \tag{21}$$

Under circularly polarized photoexcitation, the electron-nuclear states with M and $-M$ $(M \neq 0)$ can be differently involved in the kinetics, which is the main reason for the asymmetry of dependence $P_e(B_z)$ observed experimentally for $I = 3/2$ [13,17]. The particular case $I = 1/2$ is exceptional.

Indeed, in this case $v_{\pm1}=0$ and $U_{\pm1}=0$ [see Eqs. (12) and (19)], while v_0 and U_0 are nonvanishing. However, since $u_0^2 \propto B_z^2$ the factor U_0 is a symmetric function of B_z and the same is valid for the electron and nuclear spin polarizations as functions of B_z.

Expression (18) describing the effect of hyperfine interaction can be rewritten in the form

$$\frac{2\pi}{\hbar}\left(\frac{v_M}{2}\right)^2\left(\rho^{(M)}_{\frac12,\frac12}-\rho^{(M)}_{-\frac12,-\frac12}\right)\frac{1}{\pi}\frac{\hbar/T_{cn}}{(\hbar u_M)^2+(\hbar/T_{cn})^2}, \quad (22)$$

allowing the interpretation in the spirit of Fermi's golden rule for the probability rate

$$W_{21}=\frac{2\pi}{\hbar}|V_{21}|^2(f_1-f_2)\delta(E_2-E_1)$$

of the transition from the quantum state $|1\rangle$ to the state $|2\rangle$, where E_2 and E_1 are the energies of these states, f_2 and f_1 are their average occupations, and V_{21} is the matrix element of the perturbation operator. In Eq. (22), the role of the ideal δ-function is played by the smoothed δ-function with the damping T_{cn}^{-1}.

A. The model neglecting nuclear spin relaxation

If the nuclear spin relaxation is neglected then the set of kinetic equations reads as follows:

$$\begin{aligned}
&c_pN_{2,m}p=2c_n\left(n_-\rho^{(m+\frac12)}_{\frac12,\frac12}+n_+\rho^{(m-\frac12)}_{-\frac12,-\frac12}\right),\\
&2c_nn_{-s}\rho^{(M)}_{ss}+U'_M\left(\rho^{(M)}_{ss}-\rho^{(M)}_{-s,-s}\right)\\
&\quad+\frac{1}{2\tau_{sc}}\left(\rho^{(M)}_{ss}-\rho^{(M-2s)}_{-s,-s}\right)=\frac{c_p}{2}N_{2,M-s}p,
\end{aligned} \quad (23)$$

where

$$U'_M=\frac12\frac{v_M^2T_c}{1+\left(u_M^2T_c\right)^2} \quad \text{and} \quad \frac{1}{T_c}=c_nn+\frac{1}{\tau_{sc}}.$$

We remind the reader that, for $M=\pm(I+1/2)$, the value of u_M vanishes and, thus, U'_M is nonzero only for $|M|<I+1/2$.

Surprisingly, the Eqs. (23) have a simple magnetic-field-independent solution:

$$\begin{aligned}
&P_e=\frac{n_+-n_-}{n_++n_-}=\frac{P_iGT}{(1-\eta)n}, \quad P_c=\frac{N_+-N_-}{N_++N_-}=\frac{T_c}{\tau_c}P_e,\\
&\rho^{(M)}_{ss}=C_IN_1(1+P_c)^{J+M}(1-P_c)^{J-M},\\
&N_{2,m}=2C_IN_2(1+P_c)^{I+m}(1-P_c)^{I-m},
\end{aligned} \quad (24)$$

where $G=G_++G_-$ is the total optical generation rate of photoelectrons into the conduction band (or, equivalently, photoholes into the valence band), $P_i=(G_+-G_-)/(G_++G_-)$ is the initial degree of photoelectron spin polarization,

$$\eta=\frac{TT_c}{\tau\tau_c}, \quad \tau_c=\frac{1}{c_nn}, \quad \tau=\frac{1}{c_nN_1}, \quad \text{and} \quad \frac{1}{T}=\frac{1}{\tau}+\frac{1}{\tau_s}.$$

The factor C_I is given by

$$C_I=\frac{P_c}{(1+P_c)^{2I+1}-(1-P_c)^{2I+1}}$$

and equals $1/4$ for $I=1/2$ and $[8(1+P_c^2)]^{-1}$ for $I=3/2$.

One can see that, for the steady-state solution (24), the values $\rho^{(M)}_{ss}$ and $\rho^{(M)}_{-s,-s}$ coincide. This means that, on the one hand, the diagonal components of the commutator in Eqs. (16), (17), and (18) are switched off as if the hyperfine interaction were absent and, on the other hand, the nuclei are spin polarized and their spin polarizations in the single- and double-electron defect states coincide:

$$\frac{\sum_s\rho_{sm,sm}}{N_1}=\frac{N_{2,m}}{N_2}.$$

Since in the steady state the term $U'_M(\rho^{(M)}_{ss}-\rho^{(M)}_{-s,-s})$ in Eq. (23) vanishes, the densities of conduction-band electrons, n, and double-electron defects, N_2, satisfy equations independent of the hyperfine constant A and the magnetic field:

$$Y(Y+Z)=X, \quad (25)$$

$$\frac{1-Y}{a}\left\{Z-P_i^2\left(\frac{\tau_s}{\tau_h^*}\right)^2\frac{X^2(Z+\tau^*/\tau_{sc})}{[Z+\tau^*/\tau_{sc}+(1-Y)\tau_s/\tau_{sc}]^2}\right\}=X, \quad (26)$$

where $\tau^*=(c_nN_c)^{-1}$, $\tau_h^*=(c_pN_c)^{-1}$, $a=c_p/c_n$, and we use the dimensionless variables

$$X=\frac{G}{c_pN_c^2}, \quad Y=\frac{N_2}{N_c}=\frac{N_c-N_1}{N_c}, \quad \text{and} \quad Z=\frac{n}{N_c}. \quad (27)$$

In these notations the hole density p is given by $(Y+Z)N_c$. Equations (25) and (26) are identical to Eqs. (20) in Ref. [7] derived by neglecting electron-nuclear hyperfine interaction.

B. Approximation of unpolarized nuclei

In the limit of very short relaxation time τ_{n1} the hyperfine coupling described by Eq. (19) is broken and the nuclear effects are negligible.

At low excitation powers when the lifetime of the single-electron defect state $\tau_c=(c_nn)^{-1}$ is long compared with τ_{n1} and that of two-electron states $\tau_{c2}=(c_pp)^{-1}$ is longer than τ_{n2}, one can take the nuclei to be unpolarized and set

$$\rho^{(M)}_{\pm\frac12,\pm\frac12}=\frac{N_\pm}{2I+1}.$$

It follows then that the third terms describing in Eqs. (16) the hyperfine interaction can be replaced by

$$\begin{aligned}
\frac{\mathrm{i}}{\hbar}\sum_M[\mathcal{H}^{(M)}\hat\rho^{(M)}]_{\frac12,\frac12}&=-\frac{\mathrm{i}}{\hbar}\sum_M[\mathcal{H}^{(M)}\hat\rho^{(M)}]_{-\frac12,-\frac12}\\
&=\frac{N_+-N_-}{2\tau_{scn}},
\end{aligned}$$

where τ_{scn}^{-1} is the bound-electron spin relaxation rate induced by the nucleus and defined by

$$\frac{1}{\tau_{scn}}=\frac{2}{2I+1}\sum_M U_M. \quad (28)$$

Therefore, in this approximation the influence of nuclei is accounted for by replacing τ_{sc}^{-1} by the sum $\tau_{sc}^{-1}+\tau_{scn}^{-1}$.

It follows from the analysis of the above limiting cases that, in the experiment [13], the studied electron-nuclear system does not fall under these limiting conditions: both times τ_{n1} and

τ_{n2} are not extremely long and τ_{n1} is not extremely short. In the numerical treatment [19] time τ_{n2} was taken to be very short but time τ_{n1} was finite, in which case the theory allows for $I > 1/2$, an asymmetrical dependence of the electron polarization on the longitudinal magnetic field.

IV. HYPERFINE INTERACTION FOR A NUCLEUS WITH $I = 1/2$

In this case it is suitable to introduce the nuclear spin polarizations,

$$S_{n1} = \frac{1}{2}\sum_s \left(\rho_{s,\frac{1}{2};s,\frac{1}{2}} - \rho_{s,-\frac{1}{2};s,-\frac{1}{2}}\right) \text{ and}$$

$$S_{n2} = \frac{1}{2}\left(N_{2,\frac{1}{2}} - N_{2,-\frac{1}{2}}\right),$$

and the electron-nuclear spin correlator,

$$\Phi_{zz} = \tfrac{1}{4}\left(\rho_{\frac{1}{2},\frac{1}{2};\frac{1}{2},\frac{1}{2}} - \rho_{-\frac{1}{2},\frac{1}{2};-\frac{1}{2},\frac{1}{2}} - \rho_{\frac{1}{2},-\frac{1}{2};\frac{1}{2},-\frac{1}{2}} + \rho_{-\frac{1}{2},-\frac{1}{2};-\frac{1}{2},-\frac{1}{2}}\right).$$

In addition, hereafter we use the notations

$$S = \tfrac{1}{2}(n_+ - n_-) \quad \text{and} \quad S_c = \tfrac{1}{2}(N_+ - N_-)$$

for the spin polarizations of free and bound electrons.

Then the set of equations for n, N_1, N_2, p, S, S_c, S_{n1}, S_{n2}, and Φ_{zz} reduces to

$$N_1 + N_2 = N_c, \tag{29a}$$

$$p = n + N_2, \tag{29b}$$

$$c_n(nN_1 - 4SS_c) = G, \tag{29c}$$

$$c_p p N_2 = G, \tag{29d}$$

$$c_n(N_1 S - nS_c) + \frac{S}{\tau_s} = \frac{P_i}{2}G, \tag{29e}$$

$$c_n(nS_c - N_1 S) + \frac{S_c}{\tau_{sc}} + U_0(S_c - S_{n1}) = 0, \tag{29f}$$

$$\left(c_n n + \frac{1}{\tau_{sc}} + \frac{1}{\tau_{n1}}\right)\Phi_{zz} - c_n S S_{n1} = 0, \tag{29g}$$

$$c_n(nS_{n1} - 4S\Phi_{zz}) + \frac{S_{n1}}{\tau_{n1}} - U_0(S_c - S_{n1}) = c_p p S_{n2}, \tag{29h}$$

$$c_p p S_{n2} + \frac{S_{n2}}{\tau_{n2}} = c_n(nS_{n1} - 4S\Phi_{zz}), \tag{29i}$$

where U_0 is given by Eq. (19) for $M = 0$.

By using Eqs. (29g) and (29i) we can first express Φ_{zz} and S_{n2} via S_{n1} as follows:

$$\Phi_{zz} = c_n T_{cn} S S_{n1} \quad \text{and} \quad S_{n2} = \frac{c_n n - 4c_n^2 T_{cn} S^2}{c_p p + \frac{1}{\tau_{n2}}} S_{n1},$$

and then, by using Eq. (29h), we present the term $U_0(S_c - S_{n1})$ in Eq. (29f) in the form $U_0 S_c/(1 + U_0 T_N)$, where

$$\frac{1}{T_N} = \frac{1}{\tau_{n1}} + \frac{1}{\tau_{n2}}\frac{c_n n - 4c_n^2 S^2 T_{cn}}{c_p p + \frac{1}{\tau_{n2}}}. \tag{30}$$

Thus, the complete set (29) has been reduced to the set of five equations, Eqs. (29a)–(29e), together with the equation

$$c_n(nS_c - N_1 S) + \frac{S_c}{\tau_{sc}^{\text{eff}}} = 0, \tag{31}$$

where

$$\frac{1}{\tau_{sc}^{(\text{eff})}} = \frac{1}{\tau_{sc}} + \frac{U_0}{1 + U_0 T_N}. \tag{32}$$

We see that the influence of the hyperfine coupling can be described by the model derived by neglecting the nuclear effects but using the effective spin relaxation time (32), instead of the time τ_{sc}. It is worth noting that the effective time can be rewritten in the form postulated in Ref. [13]:

$$\frac{1}{\tau_{sc}^{(\text{eff})}} = \frac{1}{\tau_{sc}} + \frac{U_0}{1 + U_0 T_N} = \frac{1}{\tau_{sc}} + \frac{1}{\tau_{sc}^{(1)}}\frac{1}{1 + (\beta/\beta_{1/2})^2}, \tag{33}$$

where

$$\frac{1}{\tau_{sc}^{(1)}} = \frac{1}{T_N}\frac{\Omega^2}{\Omega^2 + \frac{2}{T_N T_{cn}}} \text{ and } \beta_{1/2} = \sqrt{\frac{\mathrm{T_N}}{2\mathrm{T_{cn}}}\left(\Omega^2 + \frac{2}{\mathrm{T_N T_{cn}}}\right)}. \tag{34}$$

It should be stressed, however, that in Eq. (34) the parameters $\tau_{sc}^{(1)}$ and $\beta_{1/2}$ are not constants but dependent on n, p, and S; they are found self-consistently during the solution procedure.

In the model under study, the magnetic field affects the electron polarization only via the time $\tau_{sc}^{(\text{eff})}$ through the field dependence of $u_0^2 = (g\mu_B B_z/\hbar)^2$. This clearly demonstrates that, for $I = 1/2$, the degree of electron spin polarization $P_e = (n_+ - n_-)/(n_+ + n_-)$ is a symmetric function of B_z, as has been stated before.

The following procedure is used to solve the set of equations (29a)–(29e) and (31) for n, p, N_1, N_2, S, and S_c. First of all we consider Eqs. (29c) and (29f) as a system of two linear equations for N_1 and S_c. The solution is represented as

$$N_1 = \frac{G}{2c_n n} R_{N_1} \quad \text{and} \quad S_c = \frac{G}{2c_n n} R_c, \tag{35}$$

where the dimensionless coefficients R_{N_1} and R_c are functions of n, p, and S. The unknown values of n, p, S, and N_2 can readily be expressed via Y and Z [see Eq. (27)] and the electron polarization degree $P_e = 2S/n$. Equation (29d) rewritten for the dimensionless variables Y and Z is given by Eq. (25). Using Eq. (35) we reduce Eq. (29e) to

$$X\left(\frac{1}{2}R_{N_1}P_e - R_c\right) + \frac{\tau_h^*}{\tau_s}P_e Z = P_i X. \tag{36}$$

To obtain the third equation we use Eqs. (29c) and (29e), express N_1 via n, P_e, G, and substitute the expression into Eq. (29a). This leads to

$$Y = 1 - a\frac{X(1 - P_i P_e) + (\tau_h^*/\tau_s)ZP_e^2}{Z\left(1 - P_e^2\right)} = \frac{\mathcal{L} + \mathcal{M}Z}{Z}, \tag{37}$$

where $\mathcal{L}$ and $\mathcal{M}$ are independent of Z. Therefore, the substitution of Eq. (37) into Eq. (25) gives a third-order equation for Z. Two of the three solutions of this equation are positive and define the dependencies of electron concentration on P_e and X. These dependencies together with Eq. (36) allow us to find two values of P_e at a fixed photogeneration rate X. One of the solutions gives a negative value of the density of the double-electron defects Y, and hence the other is a unique solution of Eqs. (25)–(37).

V. RESULTS OF COMPUTER CALCULATION AND DISCUSSION

The signature of the electron-nuclear hyperfine coupling in single-electron defect states is a growth of the spin polarization P_e of conduction-band electrons and the interband PL intensity J with increasing the longitudinal magnetic field as shown in Figs. 1(a)–1(c). In experiment this is observed, under circularly polarized interband optical excitation, via the magnetic-field-induced increase in the PL circular polarization and intensity [13,14,16,17,19]. The set of parameters unrelated to the nuclei and hyperfine coupling is the same as that used in the previous analysis [13]: $\tau^*= 2$ ps, $\tau_h^* = 30$ ps, $\tau_s = 140$ ps, $\tau_{sc} = 700$ ps, $P_i = 0.13$, and $N_c = 3\times10^{15}\,\mathrm{cm}^{-3}$. For deep centers in GaAsN the average hyperfine constant A was estimated as $6.9\times10^{-2}\,\mathrm{cm}^{-1} = 8.5\,\mu$eV [12,18]. For the nucleus with $I = 3/2$, the hyperfine splitting of the states with the total angular momenta 2 and 1 equals $2A$. To have a comparable strength of the hyperfine interaction for the nucleus with $I = 1/2$ we take $A = 17$ μeV. The choice of the nuclear spin relaxation time in the single-electron defect state, τ_{n1}, causes the greatest difficulties. Apparently, this phenomenological time parameter cannot be shorter than the time τ_{n2} describing spin relaxation of the nuclei in the two-electron defect states. The growth of the polarization P_e illustrated in Fig. 1 is calculated for (a) the coinciding times τ_{n1} and τ_{n2} and for (b) the short time τ_{n2} and the long time τ_{n1}.

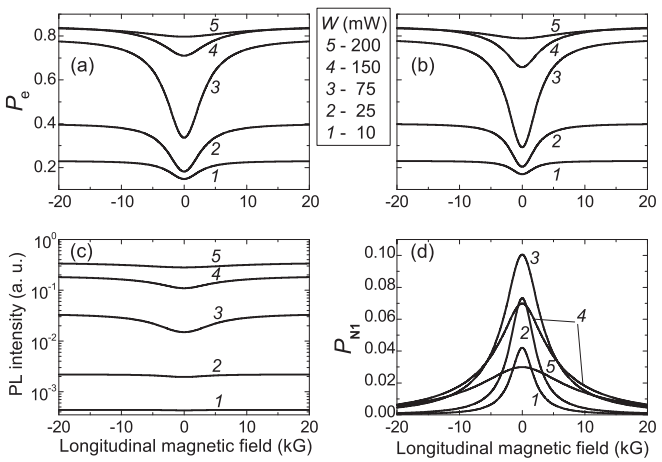

FIG. 1. Spin polarization degree of the conduction-band electrons (a,b), the intensity of interband PL (c), and nuclear spin polarization P_{N1} (d) as a function of the longitudinal magnetic field calculated for different excitation powers W of the circularly polarized light. The curves 1–5 correspond, respectively, to the following values of W: 10, 25, 75, 150, and 200 mW. The following set of model parameters is used in the calculations: $\tau^* = 2$ ps, $\tau_h^* = 30$ ps, $\tau_s = 140$ ps, $\tau_{sc} = 700$ ps, $P_i = 0.13$, $N_c = 3\times10^{15}\,\mathrm{cm}^{-3}$, and $A = 17$ μeV. The relation $G = 2\times10^{23}W$ between the generation rate and excitation power is derived from the experiment, the units for G and W are $\mathrm{cm}^{-3}\mathrm{s}^{-1}$ and mW, respectively. In panel (a), both the nuclear spin relaxation time of the one-electron defect state (τ_{n1}) and that of the two-electron state (τ_{n2}) are taken to equal 150 ps. In panels (b), (c), and (d), $\tau_{n1} = 1000$ ps and $\tau_{n2} = 1$ ps. Note that the sets of calculated curves in panels (a) and (b) s are qualitatively similar.

The nuclear spin polarization is characterized by the two polarization degrees

$$P_{N1} = \frac{1}{N_1}\sum_s \left(\rho_{s,\frac{1}{2};s,\frac{1}{2}} - \rho_{s,-\frac{1}{2};s,-\frac{1}{2}}\right) \quad \text{and}$$

$$P_{N2} = \frac{N_{2,\frac{1}{2}} - N_{2,-\frac{1}{2}}}{N_2}\,.$$

The variation of the nuclear polarization P_{N1} with the longitudinal magnetic field is illustrated in Fig. 1(d).

The dependence of nuclear polarizations P_{N1} and P_{N2} on the excitation power W calculated in the absence of magnetic field is depicted in Fig. 2. In Fig. 2(a) the values P_{N1} and P_{N2} are different but comparable in magnitude, whereas in Fig. 2(b), as expected, the polarization P_{N2} is small and the polarization P_{N1} is of the same order as the polarizations in Fig. 2(a). As seen in Fig. 1(d), the average nuclear spin is the highest at $B = 0$ and exhibits depolarization with the increasing magnetic field since the field decouples the electron and nuclear spins. It is also worth noting that the zero-field nuclear spin polarization is a nonmonotonic function of the excitation power and reaches a maximum for the intermediate power. This can be understood as follows: in the low-power

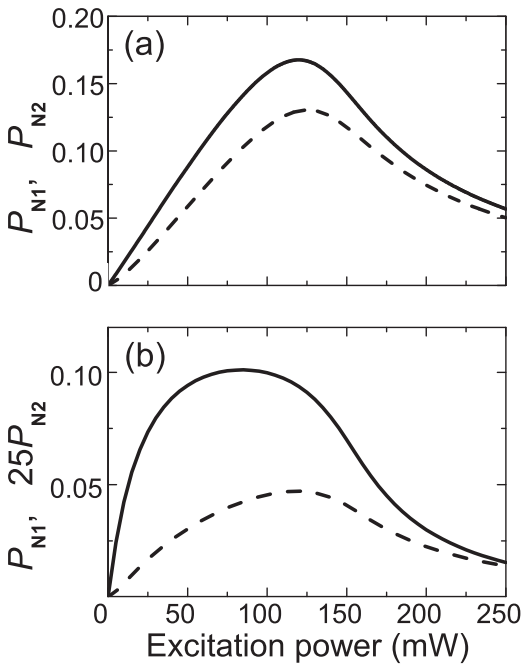

FIG. 2. Nuclear spin polarization degrees P_{N1} (solid curves) and P_{N2} (dashed) as functions of the excitation power calculated at zero magnetic field for (a) $\tau_{n1} = \tau_{n2} = 150$ ps and (b) $\tau_{n1} = 1000$ ps and $\tau_{n2} = 1$ ps. In panel (b) the values of P_{N2} are multiplied by a factor of 25.

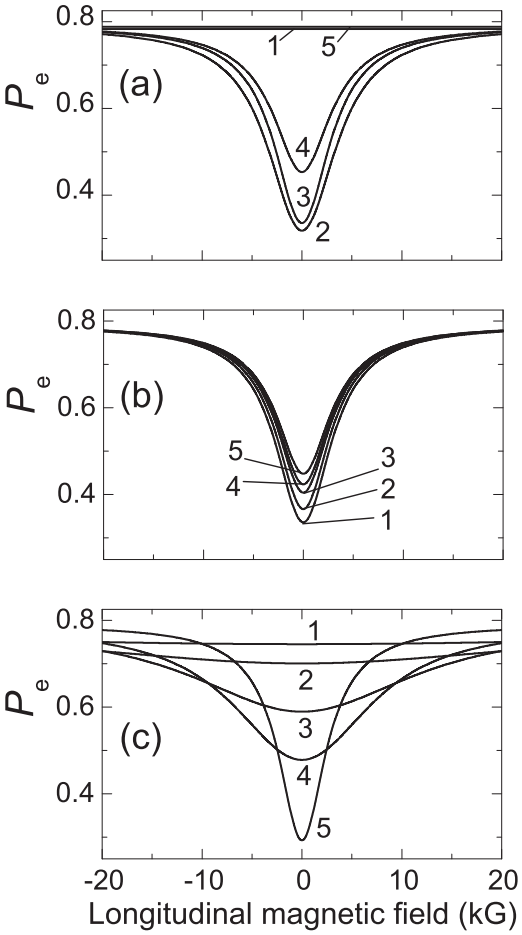

FIG. 3. Dependence of the spin polarization of the conduction-band electrons on the magnetic field calculated for the excitation power 75 mW and different values of the nuclear spin relaxation time τ_{n1} (a) assuming τ_{n1} and τ_{n2} coincide and being equal to 0.15 ps (curve 1), 50 ps (2), 150 ps (3), 450 ps (4), and 150 000 ps (5); (b) keeping $\tau_{n2} = 150$ ps fixed and taking τ_{n1} to equal 150 ps (curve 1), 300 ps (2), 750 ps (3), 1500 ps (4), and 150 000 ps (5); and (c) $\tau_{n2} =$ 1 ps and $\tau_{n1} = 1$ ps (curve 1), 2 ps (2), 5 ps (3), 10 ps (4), and 1000 ps (5). Other parameters are the same as those in Fig. 1.

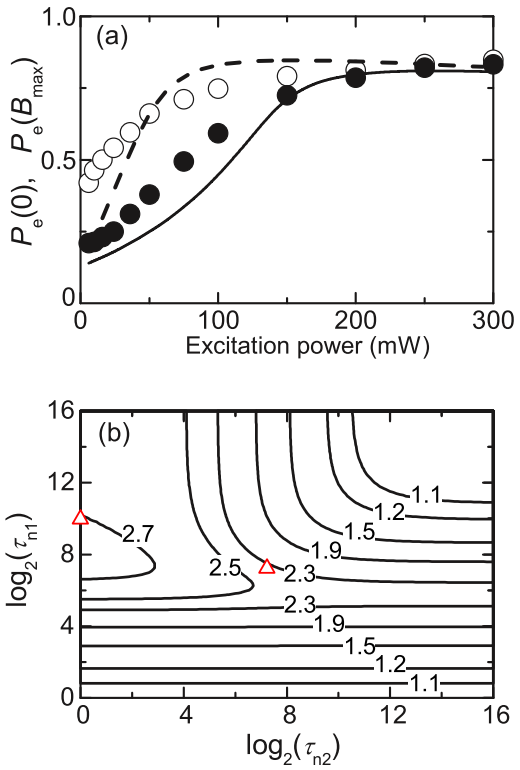

FIG. 4. (Color online) (a) Spin polarization of the conduction-band electrons as a function of the excitation power calculated at zero magnetic field (solid curve) and infinitely high magnetic field (dashed curve). The parameters are the same as those in Fig. 1(a). Solid and open circles represent the values measured in the absence of the magnetic field and at $B = 6.5$ kG [13]. (b) Isolines of the constant ratio $P_e(B \to \infty)/P_e(0)$ considered as a function of two variables, $\log_2(\tau_{n1})$ and $\log_2(\tau_{n2})$, and calculated at the excitation power $W = 75$ mW. The times τ_{n1} and τ_{n2} are in picoseconds.

limit, the system is slightly driven out of the equilibrium and the nuclear polarization is still weak; in the high-power limit, the lifetime of bound electrons τ_c is very short, the hyperfine-coupling factor U_M in Eqs. (18) and (19) decreases, and the dynamic nuclear polarization by the polarized electrons is strongly weakened.

Figure 3 illustrates the sensitivity of the polarization P_e to variation of the nuclear spin relaxation time in the models with $\tau_{n1} = \tau_{n2}$ and $\tau_{n1} \neq \tau_{n2}$. It is clear from the figure that there exists a critical interval of the time values above which the electron polarization ceases to depend on the magnetic field, confirming the conclusion of Sec. III A. The detailed calculation shows that this interval lies around 1000 ps. On the other hand, at extremely short nuclear spin relaxation times τ_{n1} the magnetic field dependence of P_e disappears as well, due to the increasing uncertainty of T_{cn} in Eqs. (19) and (20).

The spin-filtering effect is demonstrated in Fig. 4(a). At very low excitation intensity this effect is not switched on, the degree P_e is independent of the magnetic field, and the two curves in the figure calculated at zero (solid) and the infinitely high (dashed) magnetic field merge as $W \to 0$. At very high pumping the curves again merge since the lifetime T_{cn} [see Eq. (20)] becomes very short and the uncertainty caused by this reduction suppresses the hyperfine interaction. The curves in Fig. 4(a) satisfactorily reproduce the experiment data represented by circles and taken from Fig. 4(a) in Ref. [13]. An efficient characteristic of the nuclear effect is the difference from unity of the ratio

$$\zeta = \frac{P_e(\infty)}{P_e(0)} \tag{38}$$

between the degrees of free electron polarization at infinitely high and zero magnetic fields. Clearly, the values of ζ lie between 1 and $P_e^{-1}(0)$.

The ratio (38) is an intricate function of the nuclear relaxation times τ_{n1} and τ_{n2}. Figure 4(b) summarizes the calculation of this ratio and presents its isolines on the two-dimensional graph. The values 2.35 and 2.70 of ζ for the parameters used in the calculation of curve 3 in Figs. 1(a) and 1(b) are indicated by triangles in Fig. 4(b). This two-dimensional graph agrees with expectations following from the analysis of limiting cases. According to Eqs. (30) and (32), with increasing the times τ_{n1}

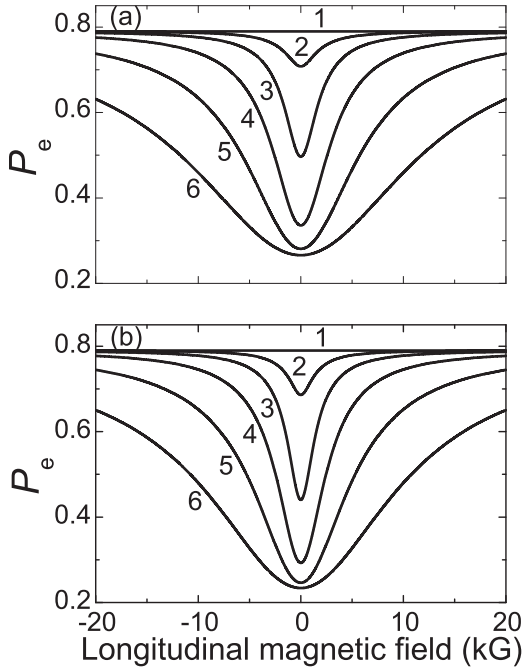

FIG. 5. Effect of the hyperfine interaction on the dependence of the spin polarization of the conduction-band electrons on the magnetic field. Curves 1–6 are calculated for the excitation power 75 mW and the following values of the hyperfine constant: $A = 0$ (horizontal line 1), $A_0/4$ (curve 2), $A_0/2$ (3), A_0 (4), $2A_0$ (5), and $4A_0$ (6), where $A_0 = 17$ μeV. In panel (a), $\tau_{n1} = \tau_{n2} = 150$ ps. In panel (b), $\tau_{n1} = 1000$ ps and $\tau_{n2} = 1$ ps. The values of the other parameters are the same as those in Fig. 1.

and τ_{n2}, the time T_N tends to infinity; the effective time $\tau_{sc}^{(\mathrm{eff})}$ tends to τ_{sc}; the dynamic nuclear polarization has no effect on the steady-state values of n, N_1, S, S_c, and P_e; and the ratio ζ approaches unity [see the upper-right corner of the graph in Fig. 4(b)]. This also agrees with the general conclusion of Sec. III A. In the limit of short times τ_{n1} the coupling strength U_0 vanishes, which explains the near-unity values of ζ in the bottom area of the graph. In the limit of short times τ_{n2}, the dependence of T_N on τ_{n2} saturates and Eq. (30) reduces to

$$\frac{1}{T_N} = \frac{1}{\tau_{n1}} + c_n n - 4c_n^2 S^2 T_{cn}. \tag{39}$$

Figure 4(b) shows that, except for the upper-right and bottom areas, the magnetic field strongly affects the electron polarization and causes an increase of the latter by a factor of 2 or more. Another point to be mentioned is a weak dependence of ζ on τ_{n1} and τ_{n2} outside the above two areas. Clearly, the hyperfine interaction manifests itself via the time T_N, which is a combination of times τ_{n1} and τ_{n2}, rather than via each of them separately.

Finally, Fig. 5 depicts the magnetic field dependence of P_e for different values of the hyperfine constant A. At zero A the. electron polarization is insensitive to the longitudinal magnetic field. With A increasing up to 68 μeV, the zero-field value of P_e decreases by a factor of $\sim$3. The half width $B_{1/2}$ of the recovery curve

$$\frac{P_e(B) - P_e(0)}{P_e(\infty) - P_e(0)}$$

increases sublinearly and is more sensitive to the variation of A as compared to $P_e(0)$.

VI. CONCLUSION

Thus, due to the axial symmetry of the system in the external longitudinal magnetic field, the components $\rho_{sm,s'm'}$ of the spin-density matrix of the defect state with a single electron are nonzero only for the equal total angular momentum projections $M = s + m$ and $M' = s' + m'$, and the spin-density matrix of the defect in the two-electron singlet state is diagonal and described by the densities $N_{2,m}$ of the centers with the nuclear spin projection m. The off-diagonal components $\rho_{s,M-s;s',M-s'}$ with $s \neq s'$ can be readily expressed via the diagonal components, which has allowed us to derive the quantum master equations containing only the diagonal components $\rho_{sm,sm}$ and $N_{2,m}$. The equations take into account the Zeeman splitting of the electron states in the longitudinal magnetic field, the electron-nuclear spin coupling described by the hyperfine constant A, the spin relaxation of free and bound electrons described, respectively, by the times τ_s and τ_{sc}, and the nuclear spin relaxation times τ_{n1} and τ_{n2} in the defect states with one and two electrons, respectively. The model reproduces the magnetic-field-induced suppression of the hyperfine interaction, the recovery of the electron spin polarization, and the increase in the edge PL intensity under the circularly polarized optical excitation. The dynamic nuclear spin polarization appears to be a nonmonotonic function of the excitation power. It has been shown that for the nuclear spin $I = 1/2$ both the PL intensity and the circular polarization are even functions of the longitudinal magnetic field B_z. Moreover, even for $I > 1/2$, there is no shift of the polarization-field curve or the intensity-field curve if the nuclear spin relaxation is negligible or too fast.

For $I = 1/2$ we have calculated the magnetic-field and excitation-power dependencies of the electron and nuclear spin polarizations and analyzed the role of the nuclear spin relaxation in each of the two defect states. For this purpose we have plotted contour lines of the ratio $P_e(B \to \infty)/P_e(0)$ in the two-dimensional plane $[\log_2(\tau_{n1}), \log_2(\tau_{n2})]$.

ACKNOWLEDGMENTS

This research was supported by the Russian Foundation for Basic Research (Grant No. 14-02-00959) and by the Government of Russia (Project No. 14.Z50.31.0021). We are grateful to K. V. Kavokin, M. Yu. Petrov, A. Yu. Shiryaev, M. M. Afanasiev, and L. S. Vlasenko for helpful discussions.

[1] V. K. Kalevich, E. L. Ivchenko, M. M. Afanasiev, A. Yu. Shiryaev, A. Yu. Egorov, V. M. Ustinov, B. Pal, and Y. Masumoto, Pis'ma Zh. Eksp. Teor. Fiz. **82**, 509 (2005) [JETP Lett. **82**, 455 (2005)].

[2] V. K. Kalevich, A. Yu. Shiryaev, E. L. Ivchenko, A. Yu. Egorov, L. Lombez, D. Lagarde, X. Marie, and T. Amand, Pis'ma Zh. Eksp. Teor. Fiz. **85**, 208 (2007) [JETP Lett. **85**, 174 (2007)].
[3] X. J. Wang, Y. Puttisong, C. W. Tu, Aaron J. Ptak, V. K. Kalevich, A. Yu. Egorov, L. Geelhaar, H. Riechert, W. M. Chen, and I. A. Buyanova, Appl. Phys. Lett. **95**, 241904 (2009).
[4] F. Zhao, A. Balocchi, A. Kunold, J. Carrey, H. Carrère, T. Amand, N. Ben Abdallah, J. C. Harmand, and X. Marie, Appl. Phys. Lett. **95**, 241104 (2009).
[5] F. Zhao, A. Balocchi, G. Truong, T. Amand, X. Marie, X. J. Wang, I. A. Buyanova, W. M. Chen, and J. C. Harmand, J. Phys.: Condens. Matter **21**, 174211 (2009).
[6] Y. Puttisong, X. J. Wang, I. A. Buyanova, H. Carrère, F. Zhao, A. Balocchi, X. Marie, C. W. Tu, and W. M. Chen, Appl. Phys. Lett. **96**, 052104 (2010).
[7] E. L. Ivchenko, V. K. Kalevich, A. Yu. Shiryaev, M. M. Afanasiev, and Y. Masumoto, J. Phys.: Condens. Matter **22**, 465804 (2010).
[8] C. Weisbuch and G. Lampel, Solid State Commun. **14**, 141 (1974).
[9] D. Paget, Phys. Rev. B **30**, 931 (1984).
[10] A. Kunold, A. Balocchi, F. Zhao, T. Amand, N. B. Abdallah, J. C. Harmand, and X. Marie, Phys. Rev. B **83**, 165202 (2011).
[11] M. I. Dyakonov and V. I. Perel, Zh. Eksp. Teor. Fiz. **63**, 1883 (1972) [Sov. Phys. JETP **36**, 995 (1973)].
[12] X. J. Wang, I. A. Buyanova, F. Zhao, D. Lagarde, A. Balocchi, X. Marie, C. W. Tu, J. C. Harmand, and W. M. Chen, Nat. Mater. **8**, 198 (2009).
[13] V. K. Kalevich, M. M. Afanasiev, A. Yu. Shiryaev, and A. Yu. Egorov, Phys. Rev. B **85**, 035205 (2012).
[14] V. K. Kalevich, M. M. Afanasiev, A. Yu. Shiryaev, and A. Yu. Egorov, Pis'ma Zh. Eksp. Teor. Fiz. **96**, 635 (2012) [JETP Lett. **96**, 567 (2012)].
[15] C. T. Nguyen, A. Balocchi, D. Lagarde, T. T. Zhang, H. Carrère, S. Mazzucato, P. Barate, E. Galopin, J. Gierak, E. Bourhis, J. C. Harmand, T. Amand, and X. Marie, Appl. Phys. Lett. **103**, 052403 (2013).
[16] Y. Puttisong, X. J. Wang, I. A. Buyanova, and W. M. Chen, Phys. Rev. B **87**, 125202 (2013).
[17] Y. Puttisong, X. J. Wang, I. A. Buyanova, L. Geelhaar, H. Riechert, A. J. Ptak, C. W. Tu, and W. M. Chen, Nat. Commun. **4**, 1751 (2013).
[18] Y. Puttisong, I. A. Buyanova, and W. M. Chen, Phys. Rev. B **89**, 195412 (2014).
[19] C. Sandoval-Santana, A. Balocchi, T. Amand, J. C. Harmand, A. Kunold, and X. Marie, Phys. Rev. B **90**, 115205 (2014).